Quantitative cell polarity imaging defines leader-to-follower transitions during collective migration and the key role of microtubule-dependent adherens junction formation

Revenu, Céline ; Streichan, Sebastian ; Donà, Erika ; Lecaudey, Virginie ; Hufnagel, Lars ; Gilmour, Darren

Abstract: The directed migration of cell collectives drives the formation of complex organ systems. A characteristic feature of many migrating collectives is a 'tissue-scale' polarity, whereby 'leader' cells at the edge of the tissue guide trailing 'followers' that become assembled into polarised epithelial tissues en route. Here, we combine quantitative imaging and perturbation approaches to investigate epithelial cell state transitions during collective migration and organogenesis, using the zebrafish lateral line primordium as an in vivo model. A readout of three-dimensional cell polarity, based on centrosomal-nucleus axes, allows the transition from migrating leaders to assembled followers to be quantitatively resolved for the first time in vivo. Using live reporters and a novel fluorescent protein timer approach, we investigate changes in cell-cell adhesion underlying this transition by monitoring cadherin receptor localisation and stability. This reveals that while cadherin 2 is expressed across the entire tissue, functional apical junctions are first assembled in the transition zone and become progressively more stable across the leader-follower axis of the tissue. Perturbation experiments demonstrate that the formation of these apical adherens junctions requires dynamic microtubules. However, once stabilised, adherens junction maintenance is microtubule independent. Combined, these data identify a mechanism for regulating leader-to-follower transitions within migrating collectives, based on the relocation and stabilisation of cadherins, and reveal a key role for dynamic microtubules in this process.

DOI: https://doi.org/10.1242/dev.101675

© 2014. Published by The Company of Biologists Ltd | Development (2014) 141, 1282-1291 doi:10.1242/dev.101675

RESEARCH ARTICLE

Quantitative cell polarity imaging defines leader-to-follower transitions during collective migration and the key role of microtubule-dependent adherens junction formation

Céline Revenu[§], Sebastian Streichan*, Erika Donà, Virginie Lecaudey[‡], Lars Hufnagel and Darren Gilmour[§]

ABSTRACT

The directed migration of cell collectives drives the formation of complex organ systems. A characteristic feature of many migrating collectives is a 'tissue-scale' polarity, whereby 'leader' cells at the edge of the tissue guide trailing 'followers' that become assembled into polarised epithelial tissues en route. Here, we combine quantitative imaging and perturbation approaches to investigate epithelial cell state transitions during collective migration and organogenesis, using the zebrafish lateral line primordium as an *in vivo* model. A readout of three-dimensional cell polarity, based on centrosomal-nucleus axes, allows the transition from migrating leaders to assembled followers to be quantitatively resolved for the first time *in vivo*. Using live reporters and a novel fluorescent protein timer approach, we investigate changes in cell-cell adhesion underlying this transition by monitoring cadherin receptor localisation and stability. This reveals that while cadherin 2 is expressed across the entire tissue, functional apical junctions are first assembled in the transition zone and become progressively more stable across the leader-follower axis of the tissue. Perturbation experiments demonstrate that the formation of these apical adherens junctions requires dynamic microtubules. However, once stabilised, adherens junction maintenance is microtubule independent. Combined, these data identify a mechanism for regulating leader-to-follower transitions within migrating collectives, based on the relocation and stabilisation of cadherins, and reveal a key role for dynamic microtubules in this process.

KEY WORDS: Collective migration, Morphogenesis, Microtubules, Cell adhesion, Lateral line, Zebrafish

INTRODUCTION

The coordinated remodelling of epithelial sheets drives the morphogenesis of many organ systems. Epithelial plasticity can occur through epithelial mesenchymal transitions (EMTs) and mesenchymal epithelial transitions (METs), the reversible process whereby static epithelia are broken down to form individual, motile mesenchymal cells. This full cell state conversion witnesses changes in cell shape and polarity, gene expression and signalling (Thiery et al., 2009; Lim and Thiery, 2012; Nieto, 2013). Collective migration is an alternative, but related, process whereby a subset of cells at the tissue edge, termed 'leader' cells, displays reduced apicobasal polarity and increased dynamic actin-based protrusions, but maintains stable contacts with trailing epithelial 'follower' cells (Friedl et al., 2004; Lecaudey and Gilmour, 2006). Unlike EMT, collective migration does not necessarily involve a full state conversion but rather modulates the degree of epithelial organisation, which we will refer to as increased epithelialisation (Revenu and Gilmour, 2009). Collective migration therefore allows epithelial tissues to become organised while moving. However, understanding the spatiotemporal coordination of this process has been limited by a lack of quantitative analysis of cell behaviour in these three-dimensional *in vivo* contexts (Montell, 2008).

One dynamic readout of cell organisation is provided by the relative position of the centrosome and the nucleus, which has enabled the analysis of polarity in cells cultured in two-dimensions (Théry et al., 2006; Dupin et al., 2009; Rodríguez-Fraticelli et al., 2012). Moreover, nucleus-centrosome axes provide information on the organisation of the microtubule network, which is cell type specific (Bacallao et al., 1989; Meads and Schroer, 1995; Müsch, 2004; Brodu et al., 2010; Hong et al., 2010). It is known that microtubules regulate, and are regulated by, points of cell-cell contact (Chausovsky et al., 2000; Waterman-Storer et al., 2000; Yap and Manley, 2001; Ligon and Holzbaur, 2007), raising the possibility that microtubule network organisation is regulated at the supracellular or tissue level, as has recently been shown for the actomyosin system (Martin et al., 2009; Rauzi et al., 2010). However, there are a number of *in vivo* contexts where the ablation of microtubules was reported to have little influence on adherens junctions (Jankovics and Brunner, 2006; Brodu et al., 2010; Sumigray et al., 2012), indicating that the role of microtubules in tissue-shaping remains unclear.

The zebrafish posterior lateral line primordium (pLLP) provides a useful *in vivo* model for studying the interplay between motility and tissue assembly during collective migration. While migrating, cells undergo a stereotyped switch in organisation during their transition from less organised leading region to tightly packaged, rosette-like mechanosensory organ progenitors, the proneuromasts, that are regularly deposited. Although signalling pathways that regulate migration (David et al., 2002; Haas and Gilmour, 2006; Valentin et al., 2007; Aman and Piotrowski, 2008) and rosette assembly (Lecaudey et al., 2008; Nechiporuk and Raible, 2008; Hava et al., 2009) have been identified, and some of their downstream effectors are known (Ernst et al., 2012; Harding and Nechiporuk, 2012), much less is understood about the changes in the cytoskeleton and cell-cell contacts that execute these cellular behaviours. In this work, we present a quantitative three-dimensional cell polarity imaging approach of cell dimensions and orientations across the pLLP that allows the organisation of the migrating tissue to be assessed. We integrate these data with novel live cadherin reporters to further

Cell Biology and Biophysics Unit, European Molecular Biology Laboratory, Heidelberg 69117, Germany.
*Present address: Kavli Institute For Theoretical Physics, Kohn Hall, University of California, Santa Barbara, CA 93106-4030. USA. ‡Present address: BIOSS – Centre for Biological Signalling Studies, University of Freiburg, Hauptstrasse 1, 79104 Freiburg, Germany.

[§]Authors for correspondence (revenu@embl.de; gilmour@embl.de)

Received 24 July 2013; Accepted 19 January 2014

Development (2014) doi:10.1242/dev.101675

address changes in cell adhesion across the migrating collective and demonstrate a requirement for dynamic microtubules specifically during the leader-to-follower transition.

RESULTS

Quantitative analysis of cell reorganisation defines the leader to follower transition

In order to map cell polarity and orientation across the migrating collective, we used the nucleus-centrosome axis, which provides a readout of front-rear polarity in migrating cells (Gotlieb et al., 1981; Etienne-Manneville and Hall, 2001; Gomes et al., 2005) and apicobasal polarity in epithelial cells (Rodríguez-Fraticelli et al., 2012). To achieve this, we developed methods to live label simultaneously microtubules (EMTB-3GFP), centrosomes (centrin-3BFP) and nuclei (nls-tdTomato). Mosaic expression of EMTB-3GFP allowed the segmentation of the microtubule network, its associated centrosome and nucleus of individual cells (Fig. 1). The polarity of each cell was extracted by generating vectors connecting the centre of mass of each nucleus to its corresponding centrosome. Assigning these to multiple cells provided the first quantitative information on the dimensions and orientations of cells across the primordium. As primordia at any stage show a stable configuration of a leading domain plus two or three trailing rosettes, the front-to-rear axis provides a simple and robust timeline for the organogenesis process. Therefore, cells were positioned in a reconstituted virtual primordium as a function of their distance from the leading edge, to generate a polarity map of the tissue (Fig. 1). As the exact positioning of trailing rosettes varies slightly from tissue to tissue, cells were registered to the mean position of their closest rosette centre (Fig. 1). In total, 340 cells were analysed from 127 primordia. As the average primordium comprises about 100 cells, this represents approximately three times tissue coverage.

We first used this quantitative data set to define how cell dimensions change across the tissue by analysing the nucleus-centrosome distance, i.e. the length of the polarity vectors. This revealed a progressive elongation when moving rearward from the leading edge of the tissue (Fig. 2A,B). Principal component analysis (Pincus and Theriot, 2007; Keren et al., 2008) of microtubule networks in three dimensions enabled analysis of cell body aspect ratio. EMTB labelling allows the analysis of the global cell volume while excluding the highly variable, flat, actin-based membrane protrusions. It confirmed the progressive increase in length along one cell axis, indicating that cells shift from a more spherical to an elliptical shape across the front-rear tissue axis (supplementary material Fig. S1A), consistent with the acquisition of a columnar morphology. The polarity vectors of the longest cells aligned with the migration axis of the primordium (supplementary material Fig. S1B), indicating that individual cells of the primordium become elongated in the direction of migration. However, although a global increase in length is a clear trend across the tissue, a subset of cells does not show such elongation (Fig. 2A; supplementary material Fig. S1A). One likely reason for such length heterogeneity in the forming organs is the assembly of cells into rosettes-like progenitors, which presumably constrains cell geometries. Indeed, looking at the distribution of lengths around the rosettes reveals that cells are shorter closer to the rosette centre, becoming more elongated in lateral regions (Fig. 2B; supplementary material Fig. S1C). In addition, analysing vector polar angles, which provides a measure of how ‘upright’ cells are by calculating deviation from a pole running perpendicular to the main tissue axis, shows that cells are progressively more upright towards the centre of the rosettes (Fig. 2C). Thus, cell length increases during the transition from leaders to epithelial organ progenitors with cells within the rosette assemblies showing heterogeneous lengths as they become organised in a ‘firewood stack’ configuration.

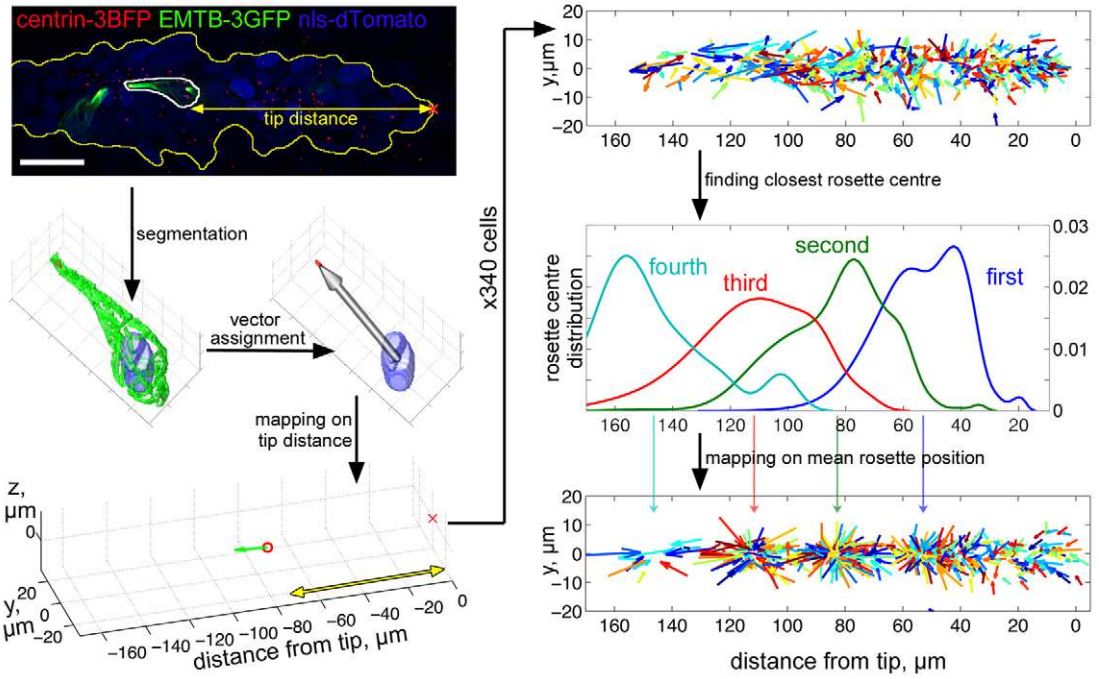

Fig. 1. Quantitative cell polarity imaging across the migrating pLLP. Data analysis pipeline used to map cellular reorganisation across the pLLP from the analysis of single cells labelled with microtubules (green), nuclei (blue) and centrosomes (red) markers. After three-dimensional segmentation, a nucleus-centrosome vector is assigned to each cell and positioned on a template pLLP as a function of the distance of the cell (yellow arrows) from the tissue leading edge (red cross). To anchor rosette positions in the map, the mean position of each rosette was used to register the nucleus-centrosome vectors to their closest rosette centre, creating an alternative data representation where the forming organs are clearly distinguished. Vectors have been assigned a random colour. Scale bar: 20 µm.

Development (2014) doi:10.1242/dev.101675

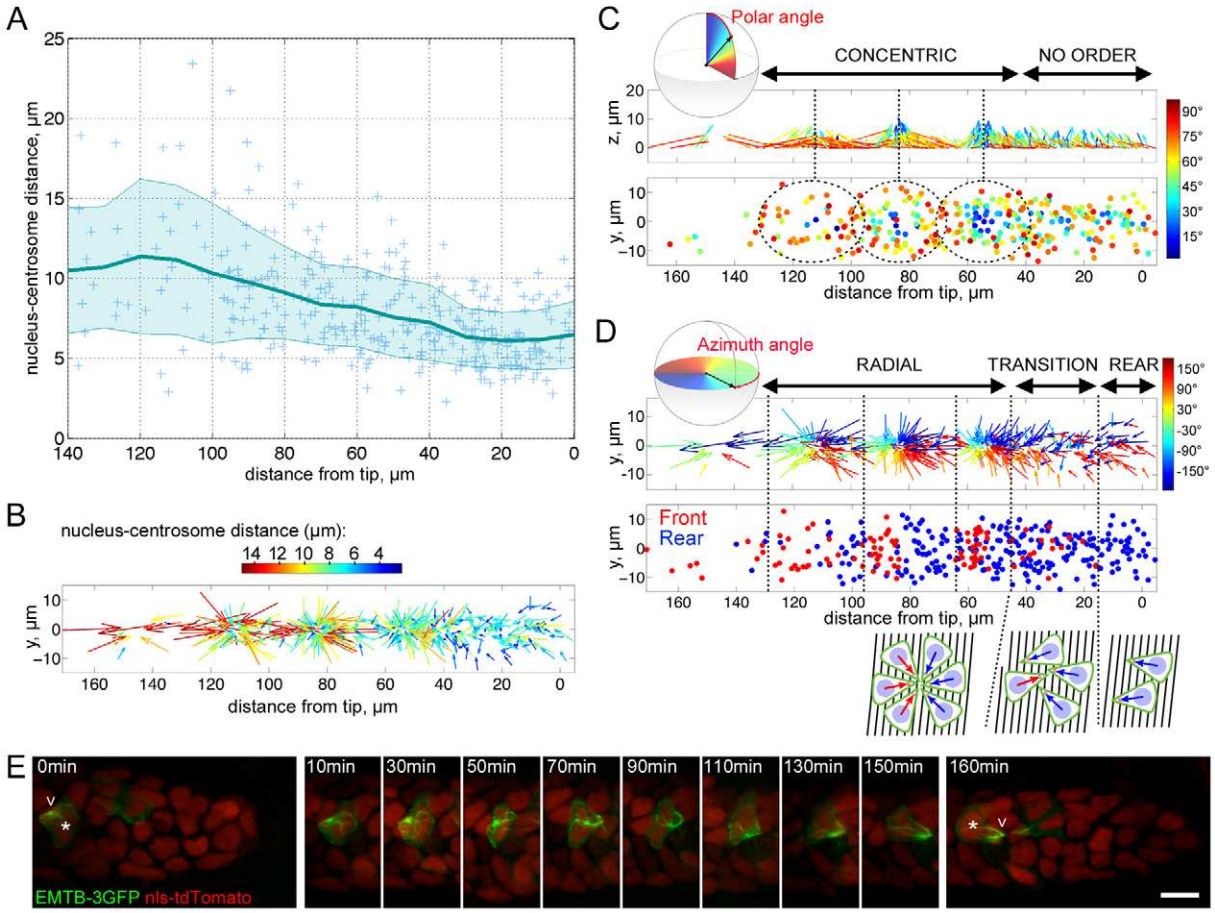

Fig. 2. Analysis of cell length and polarity changes during leader-to-follower transition. (A) Plot of the mean nucleus-centrosome distance (mean length±s.d. of the nuclear-centrosomal vectors) as a function of cell distance from the leading edge showing elongation from front to rear of the pLLP. (B) Nuclear-centrosomal vectors are colour coded according to their length, illustrating this progressive elongation. (C) Polar angles of cell polarity vectors colour coded and shown in the side view of the rosette-centred template pLLP (top) and corresponding colour coding of nuclei positions in top view (bottom). This measure of how upright cells stand shows the concentric organisation of the rosettes. (D) Polarity vectors colour coded according to their azimuth angles on a top view of the rosette-centred template pLLP (top) and plot of nuclei positions displayed in blue for rear-oriented cells and in red for front-oriented cells (bottom). This analysis of vector orientation in the migration plane demonstrates an evolution from rear-oriented to radially organised cells via a transition zone of mixed polarities. (E) Time-lapse images showing dynamically an EMTB-3GFP-expressing cell undergoing the transition from rear oriented to front oriented. The shifting cell nucleus is indicated by asterisks; chevrons indicate the brightest point of EMTB labelling that corresponds to the microtubule-organising centre. Scale bar: 10 µm.

We next addressed the direction of polarity vectors to determine how the centrosome reorients relative to the nucleus as cells become organised into rosette-like organ progenitors. The azimuth angle, i.e. the orientation of the polarity vectors in the migration plane, allowed us to quantitatively track direction changes (Fig. 2D). Azimuth angles across assembled epithelial rosettes span the whole angle range, as expected for a radial organisation. By contrast, cells within the leading 15 µm of the tissue have a strict rear orientation, meaning that cells have their centrosomes located behind the nuclei (Fig. 2D), as described for cells at the very leading edge (Pouthas et al., 2008). Front-oriented centrosomes begin to appear between 15 and 45 µm from the pLLP tip, identifying a transition zone between the leaders and the radially organised followers where centrosomal-nuclear vectors show a mixture of polarities. Performing time lapses of mosaic pLLP labelled with the microtubule marker EMTB allowed this rear-to-front shift to be dynamically confirmed at the single cell level (Fig. 2E). The transition between migrating leaders and epithelial followers is thus marked by a gradual reorientation of a subset of cell centrosomes towards the front.

Cdh2 becomes apically localised during the leader-to-follower transition

The described changes in length and orientation are likely driven by modifications in cell-cell interactions. We thus turned to cadherin-based junctions to assess whether changes in cell adhesion could explain these coordinated changes in the tissue. Previous work has shown that the pLLP expresses E-cadherin/cadherin1 (Cdh1) and N-cadherin/cadherin2 (Cdh2) (Liu et al., 2003). Anti-Cdh1 and anti-Cdh2 antibody stainings revealed co-expression of both cadherins in all cells of the pLLP (supplementary material Fig. S2A,B). Interestingly, anti-Cdh2 showed enhanced localisation to apical adherens junctions (AJs) that directly abut ZO1-labelled tight junctions (supplementary material Fig. S2C), a configuration that is a characteristic of epithelia. Surprisingly, Cdh2/*parachute* mutants show apparently normal pLLP migration and organ morphogenesis (supplementary material Fig. S2F,G), a lack of phenotype that is most likely explained by redundant expression of cadherins in the primordium (Liu et al., 2003). Nevertheless, the discrete localisation of Cdh2 makes it an excellent marker of apical AJs. In order to monitor the dynamics of AJ assembly across the migrating

Development (2014) doi:10.1242/dev.101675

primordium, we generated fluorescently tagged live reporters for Cdh2 by bacterial artificial chromosome (BAC)-mediated complementation. Transgenic lines where Cdh2 was fluorescently tagged recapitulated the pattern of endogenous Cdh2 expression (Fig. 3A; supplementary material Fig. S2D) and were able to rescue the gross morphological defects of Cdh2/*parachute* mutants, proving that these reporters were physiologically functional (supplementary material Fig. S2E). Ratiometric imaging of Cdh2 with a uniform membrane marker, lyn-GFP, confirmed a strongly enhanced apical Cdh2 localisation in cells of the rosettes (Fig. 3B,C), demonstrating that Cdh2 apical concentration is not simply the result of increased plasma membrane density. Cdh2 thus provides a live reporter for AJs across the migrating collective. Live imaging revealed that apically enriched Cdh2 first becomes detectable as discrete puncta, which then coalesce and fuse into larger multicellular clusters (Fig. 3D; supplementary material Movie 1).

Cell reorientation correlates with the formation of adherens junctions

In order to assess the link between AJ formation and cell reorientation, we quantified the localisation of Cdh2 clusters across the tissue front. Interestingly, an apical enrichment of Cdh2 was undetectable within the leading 15 µm of the tissue, with cells here instead displaying more uniform plasma membrane labelling, but appeared in the transition zone between the leading domain and the first rosette constriction (Fig. 3E). Moreover, the appearance of Cdh2 clusters shows a high spatial correlation with the percentage of front-oriented polarity vectors in the leading zone (Pearson correlation of 0.9351, Fig. 3E). Imaging of clones of cells transplanted from Cdh2-GFP- and centrin-tdTomato-expressing embryos into unlabelled hosts allowed us to follow this transition directly in single cells and suggests that cell reorientation follows Cdh2 cluster formation (Fig. 3F; supplementary material Movie 2).

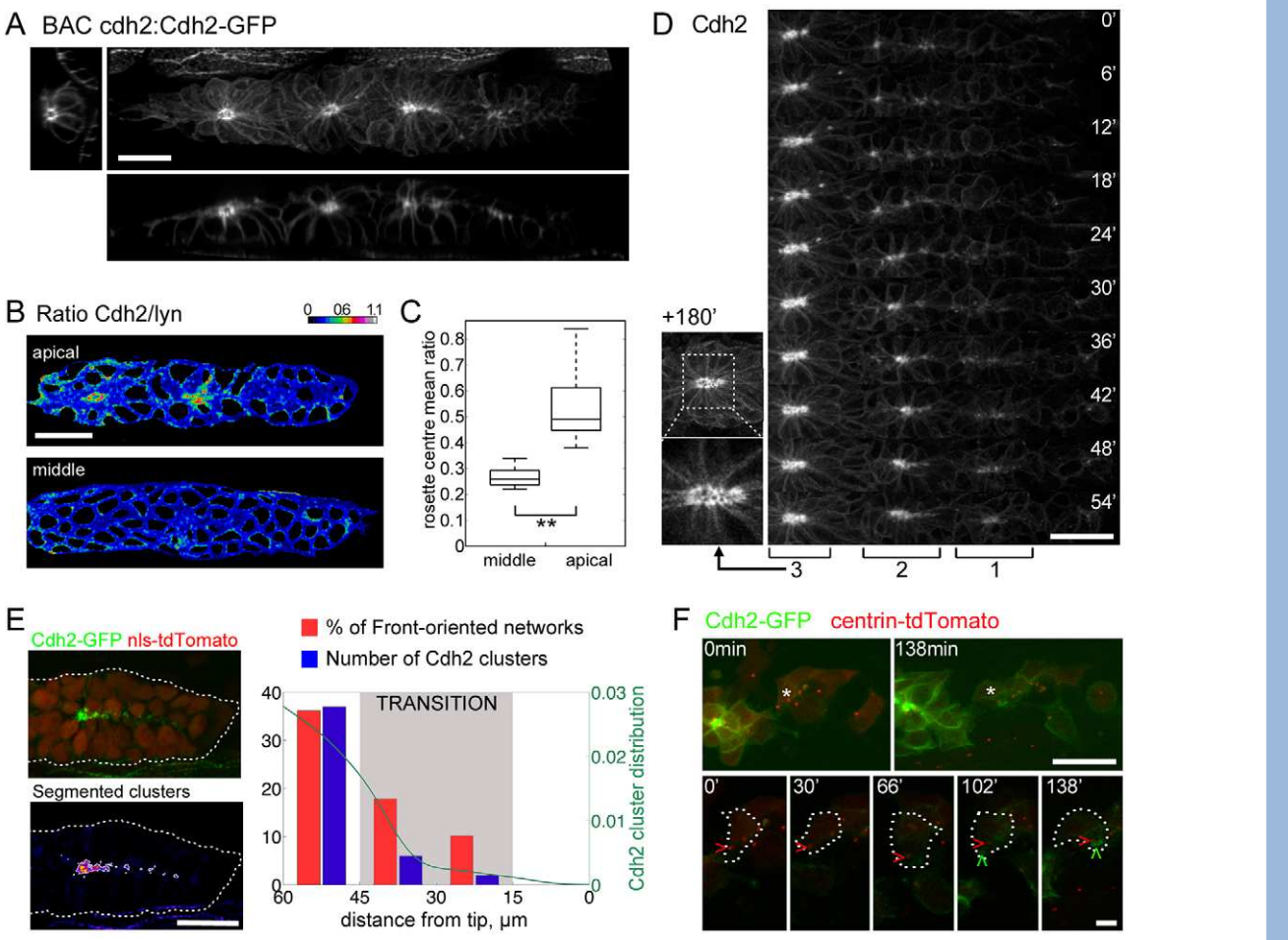

Fig. 3. Live imaging of Cdh2 reveals adherens junction assembly during organogenesis. (A) cdh2:Cdh2-GFP BAC recapitulates endogenous Cdh2 expression in the pLLP, showing enriched apical localisation of Cdh2-GFP. The maximal intensity projection of the pLLP is coupled with orthogonal *z* views. (B) Ratiometric images of cdh2:Cdh2-TagRFP and the membrane marker cldnb:lyn-GFP on confocal *z* plane show a relative increase of Cdh2 in apical rosette centres (top) that is not seen on middle *z* planes (bottom). (C) Box plots showing the distribution of the mean ratios in the rosette centre middle *z* plane and apical *z* plane (n=13, Wilcoxon paired test, $^{**}P$<0.01). (D) Concatenated time-lapse images of a Cdh2-GFP pLLP depicting (1) the appearance of apical dots just behind the leading cells and (2) the progressive clustering during rosette formation. The more mature rosette in (3) is shown on the left 3 hours later (top) together with an enlarged view of a single confocal plane (bottom) highlighting the appearance of tiny apical poles. (E) Images of Cdh2-GFP-labelled pLLP before (top) and after (bottom) segmentation of Cdh2-GFP clusters. Histogram (blue) and distribution probability (green) of segmented apical Cdh2-GFP clusters (n=27 pLLP) displayed together with the histogram of the percentage of front-oriented cells (red) in the front part of the pLLP. The transition zone defined in Fig. 2D, where front-oriented cells appear (grey) corresponds to the domain where the first apical clusters are detected. (F) Time-lapse images of Cdh2-GFP, centrin-tdTomato clones of cells in the pLLP. The indicated cell (asterisk) undergoes a transition from rear oriented to front oriented. An enlarged time-lapse view of this cell (bottom, outlined; scale bar: 5 µm) shows the appearance a Cdh2 cluster (green chevron) before the cell shifts. Red chevrons indicate the cell centrosome. Scale bars: 20 µm, unless otherwise stated.

Development (2014) doi:10.1242/dev.101675

Leader cells thus convert from a rear orientation to a radial organisation in a transition zone where cells reorient and apical AJ clusters start to form. The percentage of front-oriented cells is therefore a simple and robust proxy of epithelial organ assembly within the primordium.

Dynamic microtubules are required for apical adhesion clustering and cell radial rearrangement during the leader-to-follower transition

Having defined the cellular changes that characterise the leader-follower transition at the tissue level, we next addressed the functional requirement of the microtubule network in this morphogenesis process. We used colcemid to prevent microtubule polymerisation, the efficacy of which was confirmed by showing loss of the microtubule plus-end tracker Eb3-tdTomato (supplementary material Movie 3), and captured the response of the tissue by time-lapse imaging. Colcemid-treated primordia displayed a reproducible phenotype where organ progenitors are no longer detectable due to the loss of rosette-like constrictions (supplementary material Fig. S3A,B). In order to exclude that these morphological changes were a consequence of mitotic arrest, we blocked cells in S-phase using the DNA synthesis inhibitor aphidicolin. Aphidicolin treatment suppressed the appearance of mitotic cells but did not prevent the loss of the rosette constrictions (supplementary material Fig. S3A). UV inactivation of colcemid (supplementary material Movie 3) resulted in surprisingly efficient tissue reassembly (supplementary material Fig. S3B and Movie 4), showing that dissociated rosette organisations can rapidly return to their normal state upon microtubule regrowth. Thus, the initial assembly of rosette-like organ progenitors is tightly coupled to the status of dynamic microtubules within the collective. In order to quantify this effect, we assigned polarity vectors to 341 cells from six samples where microtubule growth was inhibited using colcemid treatment (Fig. 4A). Measuring nucleus-centrosome distances revealed that leader cells were of normal length whereas followers were shorter compared with control (Fig. 4C). This demonstrated that cell elongation during the leader-follower transition was lost upon microtubule depolymerisation. Plotting the percentage of front-oriented vectors across control primordia showed three peaks corresponding to organ progenitors (Fig. 4B). Identical analysis of cell orientation after colcemid treatment revealed that the percentage of front-oriented vectors remained low and increased sharply only at the tissue rear (Fig. 4B). Thus, although most cells are unable to become radially organised in the absence of dynamic microtubules and display a leader-like orientation, cells at the rear of the tissue maintain their multicellular organisation, suggesting that in these regions cell-cell adhesion is maintained. Indeed, complete loss of cell cohesion induced by the calcium chelator EGTA (supplementary material Movie 5), which inactivates calcium-dependent cell adhesion molecules such as cadherins, resulted in the loss of tissue organisation (Fig. 4D), as confirmed by decreased nucleus-centrosome distances along the entire primordium (Fig. 4C) and randomised orientations across the tissue (Fig. 4D). We conclude that dynamic microtubules are not essential for the cohesion of cells of the leading domain or for the integrity of mature epithelial rosettes deposited by the migrating tissue. However, there is a strict requirement for dynamic microtubules during the leader-to-follower transition.

Adherens junction stability increases across the migrating collective

In order to address the impact of microtubule depolymerisation on cadherin-based cell adhesion, we performed time-lapse analysis of Cdh2-GFP in colcemid-treated embryos (Fig. 5A). Nascent Cdh2 clusters of the transition domain no longer appeared, indicating that the initial clustering was strongly dependent on microtubules. Pre-existing Cdh2-GFP apical clusters (Fig. 5A) and ZO1 apical staining (supplementary material Fig. S3C) were lost in a front-to-rear wave (Fig. 5A), as were the rosette-like membrane constrictions (Fig. 5B). By contrast, Cdh2-GFP clusters in more mature, deposited organs proved to be refractory to microtubule depolymerisation (Fig. 5A). This increased resistance to microtubule depolymerisation towards the rear of the tissue indicates that a change in cadherin complex organisation could result in increased adhesion stability across the collective.

Work in the *Drosophila* blastoderm has shown that trans homophilic dimers of cadherin, i.e. those engaged in cell-cell junctions, are present in stable microdomains that show greatly

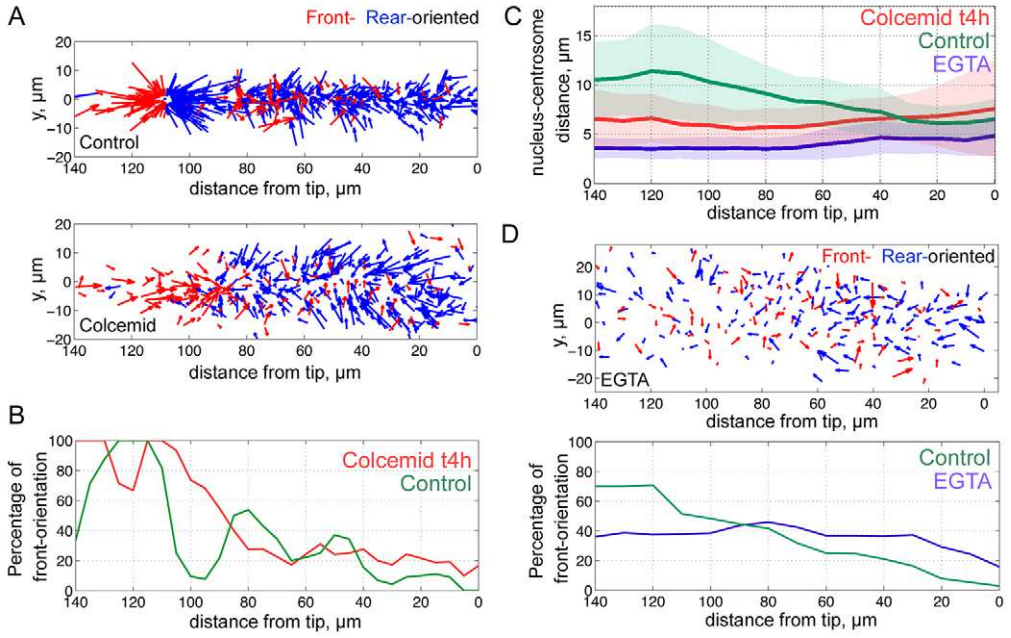

Fig. 4. Dynamic microtubules are required for epithelial organ assembly. (A) Cell polarity vectors of control and colcemid-treated cells registered on the mean last rosette position. (B) Plot of the corresponding percentage of front-oriented polarity vectors in control and colcemid-treated primordia. (C) Mean nucleus-centrosome distance (mean length±s.d. of the polarity vectors) of control and colcemid-treated cells in primordia mapped from leading-edge distance. (D) Cell polarity vectors of EGTA-treated pLLP, plotted as a function of cell distance from the leading edge and corresponding plot of the percentage of front-oriented polarity vectors across control and EGTA-treated primordia, showing the randomised orientation of cells after the loss of cell-cell contacts.

Development (2014) doi:10.1242/dev.101675

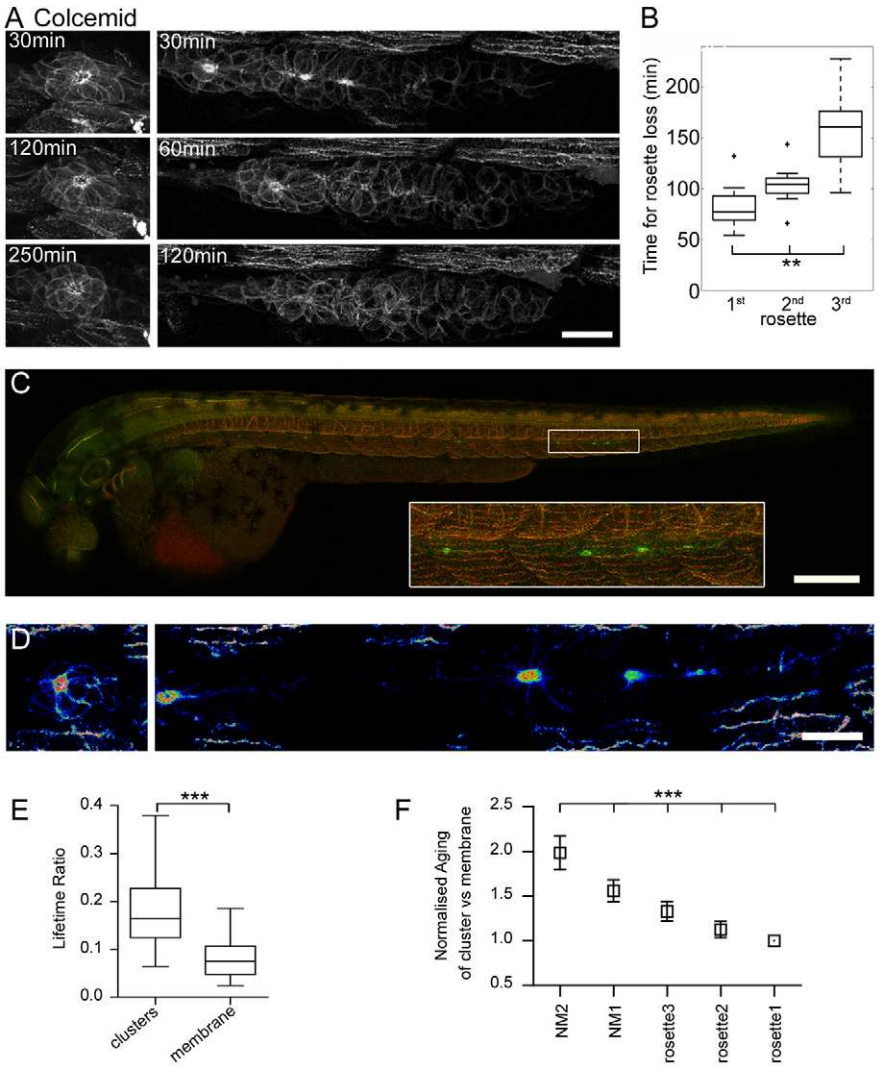

Fig. 5. Tandem fluorescent protein timers (tFTs) reveal changes in cadherin stabilisation at subcellular and tissue scales. (A) Images from a time-lapse movie showing the progressive front to rear loss of the apical Cdh2-GFP foci after colcemid treatment (right panels). A deposited neuromast maintaining Cdh2-GFP adherens junctions after colcemid treatment is shown on the left. (B) Box plots of the time required for the loss of the 1st, 2nd and 3rd rosettes after treatment with colcemid (n=12 pLLP, Friedman rank sum test, $^{**}P$<0.001). (C) BAC cdh2:Cdh2-tFTs embryo illustrating the Cdh2 age differences between tissues. Inset, magnification of the squared area containing the pLLP. Maximal intensity projections. (D) Ratiometric images of cdh2:Cdh2-tFTs show a relative increase of the red/green ratio from the front to the back pLLP rosettes and deposited neuromasts. (E) Box plots of the distribution of the lifetime ratios (red/green) of apical clusters and subjacent membranes in the corresponding area demonstrating the increased lifetime of Cdh2 in the clusters compared with membranes (n=175, paired t-test, $^{***}P$<0.001). (F) Mean and s.e.m. of the age difference between clusters and membranes (red/green ratios of clusters minus membrane) normalised on the pLLP leading most cluster (rosette1) showing a gradual stabilisation of Cdh2 in the clusters compared with membrane as rosettes mature into neuromasts (n=35 pLLP, Friedman rank sum test, $^{***}P$<0.001). NM, neuromast. Scale bars: 200 µm in C; 20 µm in A,D.

reduced mobility and turnover when compared with diffusing ‘free’ monomeric cadherin (Cavey et al., 2008). Thus, differences in the turnover of cadherin complexes provide a reasonable proxy for adhesion changes in living tissues. We therefore investigated cadherin turnover using a tandem fluorescent protein timer (tFT) methodology (Khmelinskii et al., 2012) that we have recently shown provides a quantitative readout of protein turnover within the primordium (Donà et al., 2013). We created a BAC transgenic line where Cdh2 was tagged with a tFT comprising the rapidly maturing superfolder GFP (sfGFP) and a slower maturing red fluorescent protein (TagRFP). Here, the red-over-green ratio, or lifetime ratio, allows direct evaluation of the age of the protein pool (Donà et al., 2013). Whole-mount ratiometric imaging of the Cdh2-tFT reporter revealed variable lifetime ratios between tissues (Fig. 5C). Performing lifetime ratio analysis within the primordium reveals that Cdh2-tFT is significantly older in apical clusters when compared with basolateral membranes of the same cells, confirming that these microdomains represent stabilised, hence functional, adherens junctions (Fig. 5E). We next used the same cadherin lifetime imaging approach to monitor changes in AJ stability at the tissue scale, by extracting lifetime ratios from apical clusters in multiple migrating primordia and deposited neuromasts (Fig. 5D). Quantifying their aging compared with corresponding membranes reveals that adherens junctions become progressively more stable across the front-rear axis of the collective during the formation and maturation of epithelial organ progenitors (Fig. 5F). Thus, monitoring of cadherin stability in living tissues provides a plausible mechanistic explanation for the differential requirement for dynamic microtubules during this morphogenesis process.

DISCUSSION

A common feature of many migrating collectives is the conversion of less-organised leader cells to differentiated followers that become assembled into multicellular tissues, such as tubes or rosettes. Here, we have taken a quantitative imaging approach to understand this transition in one model migrating collective: the zebrafish lateral line primordium. Through the generation of nucleus-centrosome vectors, we obtained a three-dimensional map of cell elongation and polarisation within the tissue. We characterised the conversion from leaders to epithelial mechanosensory organ progenitors and could show that cells gradually elongate and shift from a strict rear orientation, with centrosomes located between the nucleus and the cell rear, to a radial organisation in a transition zone that is concomitant with the appearance of defined apical AJs (Fig. 6). This analysis at single cell resolution provides a powerful, potentially widely applicable, approach to link subcellular and tissue-scale polarities during organogenesis.

Combining this approach with chemical perturbation experiments highlights a requirement for microtubules specifically in cells undergoing the leader-follower transition. The rapid loss of AJs in

Development (2014) doi:10.1242/dev.101675

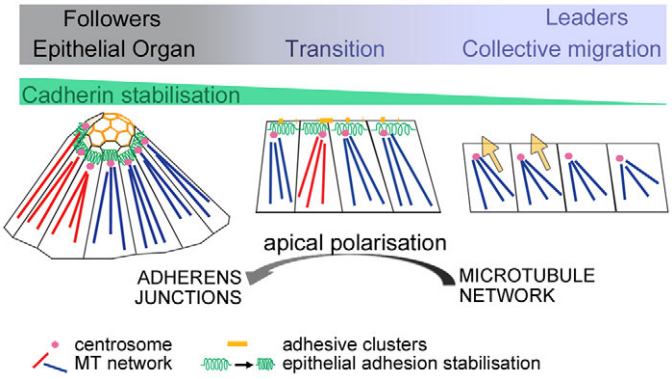

Fig. 6. Microtubule and AJ coordination of epithelial organ assembly. Model of the interactions between the microtubule network and adherens junctions in the transition from migrating leaders to differentiated epithelial followers. Microtubules promote and maintain the apical localisation of cadherin clusters. Cadherin clusters are gradually stabilised during epithelial differentiation. AJs and epithelial organisation are largely maintained in mature organs independently of the microtubule network. Early maturing adherens junctions might initiate and promote radial cell organisation during organ shaping by promoting cell reorientation.

these cells upon microtubule depolymerisation demonstrates that the microtubule network is required for the apical concentration and maintenance of the early adhesion clusters. Obviously, microtubule depolymerisation could have further effects on epithelial cell polarity than the loss of apical cadherin localisation alone, these will be the focus of future investigation. This loss of AJs is accompanied by the loss of the radial organisation, with cells mainly displaying a rear orientation typical of leader cells. Together with the tight spatial correlation between nascent AJ clusters and the reorientation of nuclear-centrosomal axes, this result suggests that forming apical cell-cell contacts could be required for cell reorientation, possibly via the microtubule network. This is an attractive hypothesis given that the position of the centrosome depends on cortical pulling forces on microtubules anchored at the cell cortex (Burakov et al., 2003) and adherens junctions are able to anchor microtubules (Ligon et al., 2001; Ligon and Holzbaur, 2007; Schmoranzer et al., 2009). Moreover, recent work has shown that shroom 3, which regulates γ-tubulin localisation and cell apico-basal elongation (Lee et al., 2007) is also localised apically in rosettes and is involved in organ progenitor formation in the pLLP (Ernst et al., 2012). As the effects of colcemid treatments are completely reversed after washout, this approach will enable future investigations into the establishment and maintenance of cell polarity within migrating tissues.

Work from a number of laboratories has shown that the centrosome is actively repositioned between the nucleus and the leading edge in cells migrating in two-dimensional cultures, a process that has been suggested to be important for directed migration (Gotlieb et al., 1981; Etienne-Manneville and Hall, 2001; Gomes et al., 2005). However, previous work has shown that when migrating cells are plated on constrained substrates, the Golgi and associated centrosome are repositioned behind the nucleus, leading to the suggestion that it could be a response to geometrical constraints (Pouthas et al., 2008). Here, we map the polarity of all nuclear-centrosomal axes across a tissue migrating *in vivo* and show that centrosomes invariably orientate towards points of cell-cell contact, as recently described in non-migrating epithelial MDCK cells plated at high density (Rodríguez-Fraticelli et al., 2012). For cells of the leading domain this results in the centrosome positioned behind the nucleus. Our finding that centrosomes are positioned towards cell-cell contacts, even in the most motile cells of the collective, indicates that these could be the dominant regulators of nuclear-centrosomal axes *in vivo*.

One surprising finding from this study is that cell-cell contacts of the collective differ strongly in their requirement for dynamic microtubules. First, cells of the leading domain remained cohesive in the absence of dynamic microtubules. Second, mature organ progenitors deposited by the migrating primordium also proved to be resistant to the effects of microtubule depolymerisation, with their apical AJs being maintained in colcemid-treated embryos. Our finding that cell states within the same migrating tissue differ strongly in their requirement of dynamic microtubules could help explain the discrepancies in studies on microtubule network regulation of AJs using different cell culture conditions or lines (Waterman-Storer et al., 2000; Yap and Manley, 2001; Ivanov et al., 2006; Ligon and Holzbaur, 2007; Komarova et al., 2012). The lack of requirement for dynamic microtubules once organ progenitors are mature indicates that AJs in these cells are stabilised through alternative mechanisms, such as changes in the actin cortex or other maturation processes. Indeed, we could show using a tandem fluorescent timer approach that Cdh2 becomes localised to clusters that become progressively more stable across the migrating tissue. This finding is of particular relevance given that cadherin complex stability can be used as a proxy for adhesion (Cavey et al., 2008). Although the cadherin-timer approach described here does not yet provide the same level of dynamic information as FRAP and photoconversion, these latter techniques require the development of time-lapse imaging and analysis protocols that are not easily applied to three-dimensional tissues. By contrast, the ‘snapshot’ nature of the cadherin-timer approach means that it can be used to monitor cadherin stability in essentially any context. For example, here we have been able to detect differences in cadherin stability at both subcellular and tissue scales using the same tandem fluorescent cadherin timer.

The conversion of leader cells to epithelial followers is expected to involve regulated changes in cell-cell adhesion. One prediction would be that cells acquire a differential Cdh1/E-cadherin and Cdh2/N-cadherin expression pattern, depending on their differentiation state (Matsuda and Chitnis, 2010), or, in analogy with METs, that cells undergo a switch in cadherin expression (Wheelock et al., 2008). Here, we show that all cells of the primordium express both Cdh1 and Cdh2, making a role for transcriptional cadherin switching unlikely in this context. Using live reporters, we demonstrate that it is the distribution of Cdh2 in the plasma membrane that changes during the transition, and, as discussed above, probably as a consequence of a local apical stabilisation of the proteins. These AJ clusters appear only in the transition zone, suggesting that leader cells have no defined apical domain and thus are more mesenchyme like in terms of organisation. High-resolution imaging of Cdh2 dynamics reveals early clusters that could be analogous to apical membrane initiation sites or pre-apical domains (Bryant et al., 2010; Yang et al., 2013) that behave like microdomains (Cavey et al., 2008). The formation of rosette-like organ progenitor could thus be driven through establishment of apical AJs, rather than the constriction of pre-existing apical domains. The existence of apical constriction is supported by the requirement for activation of actomyosin downstream of FGF and Rho-kinase during rosette formation (Ernst et al., 2012; Harding and Nechiporuk, 2012). However, there is evidence that this pathway may also act primarily in the concentration of cadherins and the formation of cell-cell junctions consistent with what we have described here (Shewan et al., 2005; Liu et al., 2010; Hoelzle and Svitkina, 2012). Given that cells of the leading domain express Cdh2, it is intriguing that they do not

Development (2014) doi:10.1242/dev.101675

show detectable apical AJs. One interesting possibility is that increased cell-matrix adhesion in these leader cells suppresses the formation of apical AJs via an integrin-cadherin negative-feedback mechanism (Ehrlich et al., 2002; Marsden and DeSimone, 2003; Sakai et al., 2003; Borghi et al., 2010; Tseng et al., 2012), an idea that could potentially explain how epithelial polarity and motility are integrated across migrating collectives.

In conclusion, this work enables us to propose a model of the transition from leaders to followers within a migrating collective (Fig. 6). Microtubules allow the apical localisation and maintenance of discrete AJ clusters in cells positioned behind the leading edge. AJs become progressively more stable as organ progenitors differentiate, with adhesion becoming independent of the dynamic microtubule network in mature deposited organs. Our work indicates that adhesive clusters could feed back on the microtubules to induce cell reorientation during the transition, an idea that will be investigated in future work. Combined, our data support a model where cell-cell adhesion within the migrating collective is primarily modulated by dynamic changes in cadherin localisation and stability, not cadherin receptor abundance. The combined quantitative analysis of cell polarity and cadherin stability described here should facilitate similar investigations into the mechanisms underlying leader-follower transitions in other *in vivo* contexts.

MATERIALS AND METHODS

Zebrafish (*Danio rerio*) lines

The previously described cldnb:lyn-GFP transgenic line (Haas and Gilmour, 2006) was used to label cell membranes of the pLLP. To visualise the microtubule cytoskeleton, we chose a mosaic expression system using a 6×UAS promoter and the GAL4-UAS:mCherry (ETL GA346) line provided by R. Köster (Distel et al., 2009). For the microtubule network, EMTB tagged with three GFPs (Bulinski et al., 1999) was cloned into a Gateway pENTR vector (Invitrogen) with *Cla*I and *Not*I restriction sites. Transgenic lines were generated using the Tol2 Kit (Kwan et al., 2007). The Cdh2 reporter lines were generated by replacing the stop codon of the cadherin 2 gene with a sequence encoding the eGFP or TagRFP fluorophore or the tandem fluorescent protein timer sfGFP-TagRFP (Donà et al., 2013) in the bacterial artificial chromosome (BAC) clone DKEYP-38F5 using standard ET recombineering technology (Gene-Bridges). The modified BACs containing a *crystallin* beta:eCFP transgenesis marker inserted in the backbone were injected in the Cdh2 mutant strain *parachute* (PAC, allele *tm101b*) (Jiang et al., 1996). To label nuclei, a BAC line expressing a nuclear localisation signal tagged with tdTomato under the Cxcr4b regulatory sequences was used (*Cxcr4b*:nls-tdTomato) (Donà et al., 2013). Mosaic embryos were generated by introducing cdh2:Cdh2-GFP cells injected with centrin-tdTomato mRNA into wild-type hosts, following previously described transplantation methods (Haas and Gilmour, 2006).

mRNA constructs and injections

All constructs were created using Multisite Gateway procedures (Invitrogen) and the SP6 promoter. Zebrafish centrin1 cDNA was cloned and fused in 5′ with the fluorescent proteins tdTomato or with three TagBFPs (Subach et al., 2008). The array of three TagBFPs was created by sequentially ligating a *Bam*HI-TagBFP-*Bgl*II PCR product into a *Bam*HI-digested pENTR vector. The human Eb3 cDNA (Stepanova et al., 2003) was fused in 3′ with tdTomato. Capped mRNAs were transcribed using the SP6 mMessage mMachine Kit (Ambion) and injected into one-cell stage embryos.

Segmentation and quantification analysis

These analyses were performed using custom codes written in MATLAB (MathWorks); scripts can be provided on request. For segmentation of individual cells, *z*-stacks with a sectioning of 500 nm were acquired using a 40× 1.2 NA water objective on PerkinElmer Improvision Ultraview spinning disc confocals (ERS and VOX) and deconvolved using Huygens Remote Manager (Ponti et al., 2007). Microtubule network, nucleus and centrosome were segmented in three dimensions using local background correction (disc size in the order of 5, 45 and 2, respectively), thresholding and Mexican hat filtering (standard deviation in the order of 0.7, 7 and 1, respectively). For the analysis of polarity vectors after drug treatments, nuclei, centrosome and membrane were segmented using the interactive machine learning Ilastik software (C. Sommer, C. Straehle, U. Köthe and F. A. Hamprecht, unpublished). Segmented nuclei and centrosome pairs were manually assigned using the microtubule network or the membrane to determine cell boundaries. To extract the position of each analysed cell in the corresponding primordium, the primordium was masked from the nuclei channel using an active contour method (Chan and Vese, 2001) to detect the orientation and the tip of the tissue. For the rosette based pLLP maps, the positions of the rosettes were manually assigned using the centrosomes and the nuclei channels or the membrane channel after colcemid treatment. For the percentage of front-oriented vectors and the mean length calculations, sliding windows of 10 and 30 µm, respectively, were used along the main tissue axis.

Immunohistochemistry

For immunohistochemistry, the following antibodies were used: mouse anti-E-cadherin (1/500; BD Transduction Laboratories), rabbit anti-cadherin 2 (1/3000) (Liu et al., 2001) and mouse anti-ZO-1 (1/200; Zymed). Approximately 32 hpf dechorionated embryos were fixed in 4% paraformaldehyde and permeabilised with PBS, 0.3% Triton X-100, 1% DMSO, 1% BSA and 0.1% Tween.

Imaging and image processing

Approximately 32 hpf embryos were anaesthetised in 0.01% tricane in E3 medium and mounted on glass-bottom Petri dishes (Mattek) with 1% low melting point agarose. Imaging was performed on PerkinElmer Improvision Ultraview spinning disc confocals (ERS and VOX) or Zeiss LSM 780 confocal using Zeiss 40× or 63× 1.2 NA water objectives. Two-photon time lapses were acquired with a Zeiss LSM 780 NLO and a 63× 1.2 NA water objective. Acquired *z*-stacks spanning the whole primordium were processed using ImageJ and Fiji software. Images shown are generally maximal intensity projections. When appropriate, subsequent fields were stitched using the pairwise stitching plug-in (Preibisch et al., 2010). For Cdh2/lyn ratio analysis, after local background subtraction, a mask of the primordium was created using the lyn-GFP channel by Gaussian filtering, thresholding and erosion. The obtained mask was then applied on the Cdh2-TRFP channel after median filtering. The resulting image was divided by the lyn-GFP one and colour-coded with the ratio look-up table. For quantifications, a region of interest of approximately 50 μm^2 of masked pixels was drawn on the rosette centre. The mean ratio was measured in a *z* plane crossing the apical concentration and 5 µm lower for each rosette. For the analysis of apical cluster distribution, Cdh2 clusters were segmented using local background subtraction, thresholding and a minimum size filter of 0.1 μm^2.

Ratiometric analysis of Cdh2 stability in apical clusters of forming and mature neuromasts

Embryos were imaged on a Zeiss LSM 780 confocal microscope as previously described (Donà et al., 2013). A *z*-stack spanning the apical clusters and a single confocal plane in the middle plane of the primordium or of the deposited neuromasts were acquired for each sample. Owing to the extreme difference in fluorescence intensities between basolateral membranes and apical constrictions, two different acquisition settings had to be used. For each acquisition setting, background and normalisation solution (sfGFP–mCherry fusion protein) images were also acquired.

After background subtraction, apical cluster and basolateral membrane regions were manually defined on individual confocal planes using the freehand line tool in Fiji (line width=0.9 µm). To calculate lifetime ratios, mean red and green fluorescence intensities were calculated and the resulting red/green ratios were normalized by the ratio of the sfGFP-mCherry reference solution (Donà et al., 2013).

To analyse the stability of Cdh2 in the clusters relative to corresponding membranes, we analysed the data as follows. For each apical cluster, the mean ratio of the underlying basolateral membrane ratio was subtracted, in

order to normalise for age differences across the anterior-posterior axis of the primordium owing to other factors affecting protein pool age, like transcription rate or cell division rate differences. For each embryo, these values were normalised to that of the front-most cluster, so that the stability of each apical cluster would be expressed relative to that one.

Drug treatments

For EGTA treatment, embryos were washed in PBS and then mounted in agarose. PBS containing 25 mM EGTA was added in the dish just before starting the acquisition. For microtubule depolymerisation, colcemid (demecolcine, Sigma) was used at 20 µg/ml in 1% DMSO final both in agarose and in E3 medium. Control embryos were treated with 1% DMSO. For rescue experiments, the medium was washed out with 1% DMSO in E3 and the embryos were irradiated with UV for 30 seconds to inactivate the drug using a 5× objective and an HBO lamp. In order to prevent entry into S phase, embryos were treated with 75 µM aphidicolin (Sigma) and 10 mM hydroxyurea in E3 containing 1% DMSO final at least 4 hours before colcemid treatment.

Acknowledgements

We are grateful to Andreea Gruia for excellent animal care and the Advanced Light Microscopy Facility for imaging support. We thank Reinhard Koester and Martin Distel for kindly providing the lateral line GAL4-driver. We thank Jan Ellenberg, Marcus Heisler, Peter Lenart and Francesca Peri for critical reading of the manuscript and the Gilmour laboratory for stimulating discussions.

Competing interests

The authors declare no competing financial interests.

Author contributions

C.R. and D.G. designed the study, aspects of the design were influenced by initial experiments performed by V.L. C.R. performed all experiments. S.S. and L.H. designed data analysis methods. C.R. and S.S. analysed and interpreted the data in discussion with D.G. E.D. assisted with cadherin-timer experiments and carried out cadherin-timer data analysis. C.R. and D.G. wrote the manuscript, incorporating feedback from all authors.

Funding

C.R. was supported by EMBO Long Term and EMBL EIPOD fellowships.

Supplementary material

Supplementary material available online at
http://dev.biologists.org/lookup/suppl/doi:10.1242/dev.101675/-/DC1

References

Aman, A. and Piotrowski, T. (2008). Wnt/beta-catenin and Fgf signaling control collective cell migration by restricting chemokine receptor expression. *Dev. Cell* **15**, 749-761.

Bacallao, R., Antony, C., Dotti, C., Karsenti, E., Stelzer, E. H. and Simons, K. (1989). The subcellular organization of Madin-Darby canine kidney cells during the formation of a polarized epithelium. *J. Cell Biol.* **109**, 2817-2832.

Borghi, N., Lowndes, M., Maruthamuthu, V., Gardel, M. L. and Nelson, W. J. (2010). Regulation of cell motile behavior by crosstalk between cadherin- and integrin-mediated adhesions. *Proc. Natl. Acad. Sci. USA* **107**, 13324-13329.

Brodu, V., Baffet, A. D., Le Droguen, P. M., Casanova, J. and Guichet, A. (2010). A developmentally regulated two-step process generates a noncentrosomal microtubule network in Drosophila tracheal cells. *Dev. Cell* **18**, 790-801.

Bryant, D. M., Datta, A., Rodríguez-Fraticelli, A. E., Peränen, J., Martín-Belmonte, F. and Mostov, K. E. (2010). A molecular network for de novo generation of the apical surface and lumen. *Nat. Cell Biol.* **12**, 1035-1045.

Bulinski, J. C., Gruber, D., Faire, K., Prasad, P. and Chang, W. (1999). GFP chimeras of E-MAP-115 (ensconsin) domains mimic behavior of the endogenous protein in vitro and in vivo. *Cell Struct. Funct.* **24**, 313-320.

Burakov, A., Nadezhdina, E., Slepchenko, B. and Rodionov, V. (2003). Centrosome positioning in interphase cells. *J. Cell Biol.* **162**, 963-969.

Cavey, M., Rauzi, M., Lenne, P. F. and Lecuit, T. (2008). A two-tiered mechanism for stabilization and immobilization of E-cadherin. *Nature* **453**, 751-756.

Chan, T. F. and Vese, L. A. (2001). Active contours without edges. *IEEE* **10**, 266-277.

Chausovsky, A., Bershadsky, A. D. and Borisy, G. G. (2000). Cadherin-mediated regulation of microtubule dynamics. *Nat. Cell Biol.* **2**, 797-804.

David, N. B., Sapède, D., Saint-Etienne, L., Thisse, C., Thisse, B., Dambly-Chaudière, C., Rosa, F. M. and Ghysen, A. (2002). Molecular basis of cell migration in the fish lateral line: role of the chemokine receptor CXCR4 and of its ligand, SDF1. *Proc. Natl. Acad. Sci. USA* **99**, 16297-16302.

Distel, M., Wullimann, M. F. and Köster, R. W. (2009). Optimized Gal4 genetics for permanent gene expression mapping in zebrafish. *Proc. Natl. Acad. Sci. USA* **106**, 13365-13370.

Donà, E., Barry, J. D., Valentin, G., Quirin, C., Khmelinskii, A., Kunze, A., Durdu, S., Newton, L. R., Fernandez-Minan, A., Huber, W. et al. (2013). Directional tissue migration through a self-generated chemokine gradient. *Nature* **503**, 285-289.

Dupin, I., Camand, E. and Etienne-Manneville, S. (2009). Classical cadherins control nucleus and centrosome position and cell polarity. *J. Cell Biol.* **185**, 779-786.

Ehrlich, J. S., Hansen, M. D. and Nelson, W. J. (2002). Spatio-temporal regulation of Rac1 localization and lamellipodia dynamics during epithelial cell-cell adhesion. *Dev. Cell* **3**, 259-270.

Ernst, S., Liu, K., Agarwala, S., Moratscheck, N., Avci, M. E., Dalle Nogare, D., Chitnis, A. B., Ronneberger, O. and Lecaudey, V. (2012). Shroom3 is required downstream of FGF signalling to mediate proneuromast assembly in zebrafish. *Development* **139**, 4571-4581.

Etienne-Manneville, S. and Hall, A. (2001). Integrin-mediated activation of Cdc42 controls cell polarity in migrating astrocytes through PKCzeta. *Cell* **106**, 489-498.

Friedl, P., Hegerfeldt, Y. and Tusch, M. (2004). Collective cell migration in morphogenesis and cancer. *Int. J. Dev. Biol.* **48**, 441-449.

Gomes, E. R., Jani, S. and Gundersen, G. G. (2005). Nuclear movement regulated by Cdc42, MRCK, myosin, and actin flow establishes MTOC polarization in migrating cells. *Cell* **121**, 451-463.

Gotlieb, A. I., May, L. M., Subrahmanyan, L. and Kalnins, V. I. (1981). Distribution of microtubule organizing centers in migrating sheets of endothelial cells. *J. Cell Biol.* **91**, 589-594.

Haas, P. and Gilmour, D. (2006). Chemokine signaling mediates self-organizing tissue migration in the zebrafish lateral line. *Dev. Cell* **10**, 673-680.

Harding, M. J. and Nechiporuk, A. V. (2012). Fgfr-Ras-MAPK signaling is required for apical constriction via apical positioning of Rho-associated kinase during mechanosensory organ formation. *Development* **139**, 3130-3135.

Hava, D., Forster, U., Matsuda, M., Cui, S., Link, B. A., Eichhorst, J., Wiesner, B., Chitnis, A. and Abdelilah-Seyfried, S. (2009). Apical membrane maturation and cellular rosette formation during morphogenesis of the zebrafish lateral line. *J. Cell Sci.* **122**, 687-695.

Hoelzle, M. K. and Svitkina, T. (2012). The cytoskeletal mechanisms of cell-cell junction formation in endothelial cells. *Mol. Biol. Cell* **23**, 310-323.

Hong, E., Jayachandran, P. and Brewster, R. (2010). The polarity protein Pard3 is required for centrosome positioning during neurulation. *Dev. Biol.* **341**, 335-345.

Ivanov, A. I., McCall, I. C., Babbin, B., Samarin, S. N., Nusrat, A. and Parkos, C. A. (2006). Microtubules regulate disassembly of epithelial apical junctions. *BMC Cell Biol.* **7**, 12.

Jankovics, F. and Brunner, D. (2006). Transiently reorganized microtubules are essential for zippering during dorsal closure in Drosophila melanogaster. *Dev. Cell* **11**, 375-385.

Jiang, Y. J., Brand, M., Heisenberg, C. P., Beuchle, D., Furutani-Seiki, M., Kelsh, R. N., Warga, R. M., Granato, M., Haffter, P., Hammerschmidt, M. et al. (1996). Mutations affecting neurogenesis and brain morphology in the zebrafish, Danio rerio. *Development* **123**, 205-216.

Keren, K., Pincus, Z., Allen, G. M., Barnhart, E. L., Marriott, G., Mogilner, A. and Theriot, J. A. (2008). Mechanism of shape determination in motile cells. *Nature* **453**, 475-480.

Khmelinskii, A., Keller, P. J., Bartosik, A., Meurer, M., Barry, J. D., Mardin, B. R., Kaufmann, A., Trautmann, S., Wachsmuth, M., Pereira, G. et al. (2012). Tandem fluorescent protein timers for in vivo analysis of protein dynamics. *Nat. Biotechnol.* **30**, 708-714.

Komarova, Y. A., Huang, F., Geyer, M., Daneshjou, N., Garcia, A., Idalino, L., Kreutz, B., Mehta, D. and Malik, A. B. (2012). VE-cadherin signaling induces EB3 phosphorylation to suppress microtubule growth and assemble adherens junctions. *Mol. Cell* **48**, 914-925.

Kwan, K. M., Fujimoto, E., Grabher, C., Mangum, B. D., Hardy, M. E., Campbell, D. S., Parant, J. M., Yost, H. J., Kanki, J. P. and Chien, C. B. (2007). The Tol2kit: a multisite gateway-based construction kit for Tol2 transposon transgenesis constructs. *Dev. Dyn.* **236**, 3088-3099.

Lecaudey, V. and Gilmour, D. (2006). Organizing moving groups during morphogenesis. *Curr. Opin. Cell Biol.* **18**, 102-107.

Lecaudey, V., Cakan-Akdogan, G., Norton, W. H. and Gilmour, D. (2008). Dynamic Fgf signaling couples morphogenesis and migration in the zebrafish lateral line primordium. *Development* **135**, 2695-2705.

Lee, C., Scherr, H. M. and Wallingford, J. B. (2007). Shroom family proteins regulate gamma-tubulin distribution and microtubule architecture during epithelial cell shape change. *Development* **134**, 1431-1441.

Ligon, L. A. and Holzbaur, E. L. (2007). Microtubules tethered at epithelial cell junctions by dynein facilitate efficient junction assembly. *Traffic* **8**, 808-819.

Ligon, L. A., Karki, S., Tokito, M. and Holzbaur, E. L. (2001). Dynein binds to beta-catenin and may tether microtubules at adherens junctions. *Nat. Cell Biol.* **3**, 913-917.

Lim, J. and Thiery, J. P. (2012). Epithelial-mesenchymal transitions: insights from development. *Development* **139**, 3471-3486.

Liu, Q., Babb, S. G., Novince, Z. M., Doedens, A. L., Marrs, J. and Raymond, P. A. (2001). Differential expression of cadherin-2 and cadherin-4 in the developing and adult zebrafish visual system. *Vis. Neurosci.* **18**, 923-933.

Liu, Q., Ensign, R. D. and Azodi, E. (2003). Cadherin-1, -2 and -4 expression in the cranial ganglia and lateral line system of developing zebrafish. *Gene Expr. Patterns* **3**, 653-658.

Liu, Z., Tan, J. L., Cohen, D. M., Yang, M. T., Sniadecki, N. J., Ruiz, S. A., Nelson, C. M. and Chen, C. S. (2010). Mechanical tugging force regulates the size of cell-cell junctions. *Proc. Natl. Acad. Sci. USA* **107**, 9944-9949.

Marsden, M. and DeSimone, D. W. (2003). Integrin-ECM interactions regulate cadherin-dependent cell adhesion and are required for convergent extension in Xenopus. *Curr. Biol.* **13**, 1182-1191.
Martin, A. C., Kaschube, M. and Wieschaus, E. F. (2009). Pulsed contractions of an actin-myosin network drive apical constriction. *Nature* **457**, 495-499.
Matsuda, M. and Chitnis, A. B. (2010). Atoh1a expression must be restricted by Notch signaling for effective morphogenesis of the posterior lateral line primordium in zebrafish. *Development* **137**, 3477-3487.
Meads, T. and Schroer, T. A. (1995). Polarity and nucleation of microtubules in polarized epithelial cells. *Cell Motil. Cytoskeleton* **32**, 273-288.
Montell, D. J. (2008). Morphogenetic cell movements: diversity from modular mechanical properties. *Science* **322**, 1502-1505.
Müsch, A. (2004). Microtubule organization and function in epithelial cells. *Traffic* **5**, 1-9.
Nechiporuk, A. and Raible, D. W. (2008). FGF-dependent mechanosensory organ patterning in zebrafish. *Science* **320**, 1774-1777.
Nieto, M. A. (2013). Epithelial plasticity: a common theme in embryonic and cancer cells. *Science* **342**, 1234850.
Pincus, Z. and Theriot, J. A. (2007). Comparison of quantitative methods for cell-shape analysis. *J. Microsc.* **227**, 140-156.
Ponti, A., Gulati, A., Bäcke, V. and Schwarb, P. (2007). Huygens remote manager: a web interface for high-volume batch deconvolution. *Imaging & Microscopy* **9**, 57-58.
Pouthas, F., Girard, P., Lecaudey, V., Ly, T. B., Gilmour, D., Boulin, C., Pepperkok, R. and Reynaud, E. G. (2008). In migrating cells, the Golgi complex and the position of the centrosome depend on geometrical constraints of the substratum. *J. Cell Sci.* **121**, 2406-2414.
Preibisch, S., Saalfeld, S., Schindelin, J. and Tomancak, P. (2010). Software for bead-based registration of selective plane illumination microscopy data. *Nat. Methods* **7**, 418-419.
Rauzi, M., Lenne, P. F. and Lecuit, T. (2010). Planar polarized actomyosin contractile flows control epithelial junction remodelling. *Nature* **468**, 1110-1114.
Revenu, C. and Gilmour, D. (2009). EMT 2.0: shaping epithelia through collective migration. *Curr. Opin. Genet. Dev.* **19**, 338-342.
Rodríguez-Fraticelli, A. E., Auzan, M., Alonso, M. A., Bornens, M. and Martín-Belmonte, F. (2012). Cell confinement controls centrosome positioning and lumen initiation during epithelial morphogenesis. *J. Cell Biol.* **198**, 1011-1023.
Sakai, T., Larsen, M. and Yamada, K. M. (2003). Fibronectin requirement in branching morphogenesis. *Nature* **423**, 876-881.
Schmoranzer, J., Fawcett, J. P., Segura, M., Tan, S., Vallee, R. B., Pawson, T. and Gundersen, G. G. (2009). Par3 and dynein associate to regulate local microtubule dynamics and centrosome orientation during migration. *Curr. Biol.* **19**, 1065-1074.
Shewan, A. M., Maddugoda, M., Kraemer, A., Stehbens, S. J., Verma, S., Kovacs, E. M. and Yap, A. S. (2005). Myosin 2 is a key Rho kinase target necessary for the local concentration of E-cadherin at cell-cell contacts. *Mol. Biol. Cell* **16**, 4531-4542.
Stepanova, T., Slemmer, J., Hoogenraad, C. C., Lansbergen, G., Dortland, B., De Zeeuw, C. I., Grosveld, F., van Cappellen, G., Akhmanova, A. and Galjart, N. (2003). Visualization of microtubule growth in cultured neurons via the use of EB3-GFP (end-binding protein 3-green fluorescent protein). *Neuroscience* **23**, 2655-2664.
Subach, O. M., Gundorov, I. S., Yoshimura, M., Subach, F. V., Zhang, J., Grüenwald, D., Souslova, E. A., Chudakov, D. M. and Verkhusha, V. V. (2008). Conversion of red fluorescent protein into a bright blue probe. *Chem. Biol.* **15**, 1116-1124.
Sumigray, K. D., Foote, H. P. and Lechler, T. (2012). Noncentrosomal microtubules and type II myosins potentiate epidermal cell adhesion and barrier formation. *J. Cell Biol.* **199**, 513-525.
Théry, M., Pépin, A., Dressaire, E., Chen, Y. and Bornens, M. (2006). Cell distribution of stress fibres in response to the geometry of the adhesive environment. *Cell Motil. Cytoskeleton* **63**, 341-355.
Thiery, J. P., Acloque, H., Huang, R. Y. and Nieto, M. A. (2009). Epithelial-mesenchymal transitions in development and disease. *Cell* **139**, 871-890.
Tseng, Q., Duchemin-Pelletier, E., Deshiere, A., Balland, M., Guillou, H., Filhol, O. and Théry, M. (2012). Spatial organization of the extracellular matrix regulates cell-cell junction positioning. *Proc. Natl. Acad. Sci. USA* **109**, 1506-1511.
Valentin, G., Haas, P. and Gilmour, D. (2007). The chemokine SDF1a coordinates tissue migration through the spatially restricted activation of Cxcr7 and Cxcr4b. *Curr. Biol.* **17**, 1026-1031.
Waterman-Storer, C. M., Salmon, W. C. and Salmon, E. D. (2000). Feedback interactions between cell-cell adherens junctions and cytoskeletal dynamics in newt lung epithelial cells. *Mol. Biol. Cell* **11**, 2471-2483.
Wheelock, M. J., Shintani, Y., Maeda, M., Fukumoto, Y. and Johnson, K. R. (2008). Cadherin switching. *J. Cell Sci.* **121**, 727-735.
Yang, Z., Zimmerman, S., Brakeman, P. R., Beaudoin, G. M., 3rd, Reichardt, L. F. and Marciano, D. K. (2013). De novo lumen formation and elongation in the developing nephron: a central role for afadin in apical polarity. *Development* **140**, 1774-1784.
Yap, A. S. and Manley, S. W. (2001). Microtubule integrity is essential for apical polarization and epithelial morphogenesis in the thyroid. *Cell Motil. Cytoskeleton* **48**, 201-212.